ACS OMEGA

http://pubs.acs.org/journal/acsodf

Article

Fabrication, Optimization, and Evaluation of Paclitaxel and Curcumin Coloaded PLGA Nanoparticles for Improved Antitumor Activity

Haiyang Hu,[⊥] Zuyue Liao,[⊥] Mengyao Xu, Shengli Wan, Yuesong Wu, Wenjun Zou,* Jianming Wu,* and Qingze Fan*

Cite This: *ACS Omega* 2023, 8, 976−986

Read Online

ACCESS | Metrics & More | Article Recommendations

ABSTRACT: Codelivery of chemotherapeutic drugs in nanoparticles can enhance the therapeutic effects against tumors. However, their anticancer properties and physiochemical characteristics can be severely influenced by many formulation parameters during the preparation process. It is a complicated development phase to select the optimal parameters for preparation of nanoparticles based on the commonly used one single parameter method, which consumes a lot of money, time, and effort, and sometimes even fails. Therefore, the statistical analysis based on Box−Behnken design (BBD) has attracted much attention in bioengineering fields because it can illustrate the influence of parameters, build mathematical models, and predict the optimal combinational factors in a decreased number of experiments. In this study, we used a three-factor three-level BBD design to optimize the preparation of poly(lactic-*co*-glycolic acid) (PLGA) nanoparticles coloaded with two anticancer drugs curcumin and paclitaxel (PLGA-CUR-PTX nanoparticles). The surfactant concentration, polymer concentration, and oil−water ratio were selected as independent variables. An optimized model of the formulation for PLGA-CUR-PTX nanoparticles was validated. The optimal nanoparticles possessed a uniform spherical shape, with an average size of 99.94 nm, and the drug encapsulation efficiencies of CUR and PTX were 63.53 and 80.64%, respectively. The drug release from nanoparticles showed a biphasic release behavior, with a release mechanism via diffusion and fundamentally quasi-Fickian diffusion. The optimized nanoparticles demonstrated an enhanced cytotoxicity effect with lower IC_{50} values to 4T1 and MCF-7 breast cancer cell lines compared to free drugs. In summary, BBD optimization of CUR and PTX coloaded nanoparticles yielded a favorable drug carrier that holds potential as an alternative treatment for anticancer therapy.

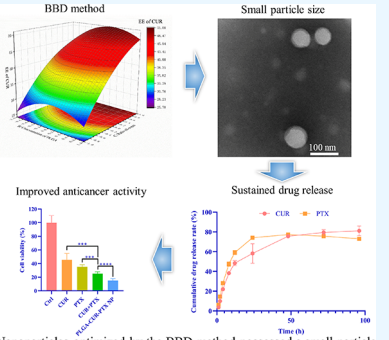

Nanoparticles optimized by the BBD method possessed a small particle size, sustained drug release and improved anticancer activity

1. INTRODUCTION

Cancer is a major public health problem worldwide, and the incidence and mortality of cancer are increasing rapidly worldwide.[1,2] Chemotherapy is the classic treatment for cancer; in particular, it can be effective in treating advanced and metastatic tumors. However, many chemotherapeutic drugs face limitations in chemotherapy, such as fast plasma clearance of drugs, severe damage to normal tissues, systemic side effects, and unsatisfactory therapeutic effects.[3] Therefore, it is a promising strategy to adopt combinational oncotherapy to reduce the dosage of chemotherapeutics to avoid side effects and to increase the antitumor efficiency.[4] Paclitaxel (PTX) is a first-line antitumor drug, which can be used to treat a variety of cancers;[5] however, it is plagued by the problems mentioned above. In the report of Madani *et al.*, paclitaxel and methotrexate (PTX/MTX) were combined for treatment of U-87 MG and B65 cells.[6] Curcumin (CUR) is extracted from the dried rhizome of *Curcuma longaL.*, which is a safe food additive and chemosensitizer and widely used in cancer therapy.[7,8] In recent years, CUR combined with MTX against glioma was reported by Mujokoro *et al.*; compared with CUR or MTX alone, CUR combined with MTX can decline the IC_{50} of CUR and MTX in U-87 MG cells.[9] CUR has been considered as a safe anticancer agent without (or with only a few) therapy-related side effects in combination with chemotherapeutic drugs such as paclitaxel, doxorubicin, and cisplatin.[10] For example, a study proved that CUR can potentiate the apoptotic effects of PTX in breast cancer cells through downregulating the gene expression of Bcl-2 and NF-κB.[11] Thus, in this study, CUR and PTX are considered as combination therapeutic agents for antitumor therapy.

Received: October 2, 2022
Accepted: December 16, 2022
Published: December 28, 2022

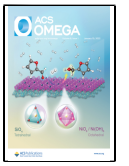

Although CUR combined with PTX is a promising strategy for cancer treatment, both drugs are confronted with the disadvantages of poor water solubility and low bioavailability, which induce unsatisfactory therapeutic effects *in vitro* and *in vivo*. To solve these problems, nanocarriers are used to coload CUR and PTX. Nanodrug carriers usually have advantages over drugs due to their nanometer size, high surface volume ratio, and good physical and chemical properties. Insoluble anticancer drugs could be encapsulated by nanoparticles to overcome the solubility and chemical stability problems of anticancer drugs and protect the anticancer drugs from being expelled and improve the circulation time of drugs *in vivo*.[12,13] Furthermore, nanoparticles could specifically target tumor areas. Due to increased vascular permeability and poor lymphatic drainage or transport in solid tumors, nanodrugs can accumulate in the tumor microenvironment, which is known as the enhanced permeability and retention (EPR) effect.[14−16] Nanoparticles could preferentially distribute on the tumor site through the EPR effect, which led to a high drug concentration in the tumor site and a low drug concentration in the normal tissue, thus enhancing the tumor treatment effect and reducing damage of chemotherapy drugs to the normal tissue.[13,17] Poly(lactic-*co*-glycolic acid) (PLGA) is an approved pharmaceutical excipient that can be processed into a nanodrug carrier for small-molecule drugs, proteins, and large-molecule drugs.[18] PLGA has attracted extensive attention as a drug carrier due to its biodegradability, protection of drug activity, and improvement of drug bioavailability.[18,19] Thus, PTX and CUR coloaded PLGA nanoparticles might be a promising strategy for increasing the antitumor efficacy and decreasing the side effects of PTX. The preparation of PLGA nanoparticles includes solvent evaporation, phase separation, spray drying, nanoprecipitation, and salting out.[18] Among these methods, solvent evaporation is the most widely used method due to its simple operation, short preparation cycle, and mature technology.

Several process variables can affect the physicochemical properties of nanocarriers, such as the size, uniformity, and drug loading efficiency, and play an important role in developing a successful nanocarrier.[20] The separate control variable method is a common method to optimize process parameters in nanoparticle preparation, which optimizes the formulation or process by changing one variable and keeping other parameters unchanged at a time (one-factor-at-time, OFAT method). Although this approach can achieve a solution for specific formulations, it does not achieve an optimal combination between process parameters.[21] In the situation of too many process parameters, this method tends to spend considerable time, money, and effort and is not conducive to repairing errors, unable to predict the optimized process parameters, and sometimes even fails.[21,22] To solve this problem, the statistical design of experiments (DoE) for optimization of nanoparticles is introduced in this study. DoE is an optimization technique method that helps to illustrate how process parameters (alone and combined) affect the product (responses). DoE can be used to optimize process variables in the preparation of nanocarriers.[23,24] The DoE methods commonly used in the fabrication of nanoparticles include screening design (such as Plackett−Burman, fractional factorial design, and full factorial design) and the response surface methodology (RSM). The RSM can build mathematical models to link response values and input process parameters.[25] The central composite design (CCD) and the Box−Behnken design (BBD) are the main RSM methods in the pharmaceutical fields. BBD is widely used in bioengineering processes because it has fewer factor levels and decreases the number of experiments.[25,26] BBD can optimize the formulation of nanocarriers through a limited number of experiments. For instance, Shaikh *et al.* successfully developed PLGA nanoparticles loaded with doxorubicin (DOX-PLGA-nanoparticles) and optimized the parameters of the nanoparticle preparation process through BBD.[27] The final obtained prescription has a small particle size (180.1 nm) and polydispersity index (PDI) (0.063), and the drug encapsulation efficiency is 52.29%.[27] Compared with the simple OFAT approach, BBD is advantageous because the statistical evaluation can provide more accurate conclusions with a reduced number of experiments.

In this study, we developed a nanomedicine consisting of CUR and PTX coloaded into PLGA nanoparticles (PLGA-CUR-PTX nanoparticles) and achieved a combination for cancer treatment. Formulation optimization was carried out through BBD on the DoE approach. The prescription attributes of PLGA-CUR-PTX nanoparticles assessed included the particle size, PDI, encapsulation efficiency, and particle morphology. The *in vitro* drug release of PLGA-CUR-PTX nanoparticles was further studied. Subsequently, the inhibition effect of cancer cells was evaluated based on the optimized prescription.

2. MATERIALS AND METHODS

2.1. Materials. Paclitaxel (PTX; degree of purity, ≥99%, BR) was procured from Dalian Meilun Biotechnology Co., Ltd., China; curcumin (CUR; degree of purity, 95%, HPLC) was procured from Shanghai Yuanye Biotechnology Co., Ltd., China; PLGA (LA/GA: 75/25, molecular weight: 30 kDa) was procured from Daigang Biological Engineering Co., Ltd., China; sodium cholate was procured from Sigma Aldrich, USA. Dichloromethane was procured from Sichuan Fairbest Technology Co., Ltd., China; phosphoric acid (degree of purity, 85−90%, HPLC) was procured from Macklin, China; acetonitrile was procured from Chengdu Hongben Chemical Products Co., Ltd., China; an ultrafiltration tube (molecular weight cutoff: 10 kDa) was procured from Millipore, USA; fetal bovine serum (FBS) was procured from MRC, USA; DMEM was procured from Gibco, USA.

2.2. Preparation and Optimization of CUR and PTX Coloaded PLGA (PLGA-CUR-PTX) Nanoparticles. *2.2.1. Preparation of PLGA-CUR-PTX Nanoparticles.* PLGA-CUR-PTX nanoparticles were developed by the emulsion solvent evaporation technique.[17] In brief, certain amounts of PTX (w/w), CUR (w/w), and PLGA were dissolved in CH_2Cl_2 as the oil phase. Subsequently, the oil phase was poured into the water phase, which consisted of a certain amount of sodium cholate, and emulsified by an ultrasonic homogenizer (Scientz-IID, Xingzhi Biological, China) in an ice bath for 2 min at 300 W to obtain the oil-in-water (O/W) emulsion. A rotary evaporation system (RV10-autopro, IKA, Germany) was used to remove CH_2Cl_2 from the emulsion in a water bath at 30 °C with a vacuum of 400 mbar and a rotating speed of 120 rpm. The nanoparticle solution was obtained after 30 min of rotary evaporation. Centrifugation (2000*g*, 5 min) was used to remove large particles from the nanoparticle solution. The nanoparticles were centrifuged at 3260*g* for 15 min, using an ultrafiltration tube, and washed three times with deionized water to obtain the purified nanoparticles. Finally,

https://doi.org/10.1021/acsomega.2c06359
ACS Omega 2023, 8, 976−986

the nanoparticles that agglomerated during the washing process were removed by centrifugation (2000*g*, 5 min), and the supernatant was taken as the final nanoparticle suspension, which was stored at 4 °C until further use.

2.2.2. Experimental Design. A Box−Behnken design (BBD) of 15 runs, three factors at three levels (3^3), with three replicates at the center point, was constructed to study the influence of different factor variables on the characteristics of PLGA-CUR-PTX nanoparticles. Experimental design and statistical analysis were performed by Design-Expert software (Design Expert 10.0.1, Stat-Ease, Minneapolis, MN, USA). The fitting formula of the quadratic model is generated by the software as follows.

$$Y = b_0 + b_1A + b_2B + b_3C + b_4AB + b_5AC + b_6BC + b_7A^2 + b_8B^2 + b_9C^2$$

where Y is the measured response, b_0 is the constant term of the polynomial equation, b_1−b_3 are linear coefficients, b_4−b_6 are interaction coefficients of the three factors, and b_7−b_9 are quadratic coefficients of the observed experimental values. The main, interacting, and quadratic effects of independent variables are *A*, *B*, and *C*; *AB*, *AC*, and *BC*; and A^2, B^2, and C^2, respectively.

In this work, three independent variables (Table 1) were chosen as follows: (A) concentration of sodium cholate (w/v, %), (B) concentration of PLGA (w/v, %), and (C) the ratio of oil volume to water volume (v/v, %). The responses to be measured (Table 2) were the (Y_1) size of nanoparticles, (Y_2) PDI of nanoparticles, (Y_3) encapsulation efficiency of CUR, (Y_4) encapsulation efficiency of PTX, and (Y_5) total encapsulation efficiency. Corresponding to the independent variables, three different levels were established as the lowest (−1), the highest (+1), and central values (0) of the tested variables (Table 1). The matrix of 15 experimental formulations was constructed as represented in Table 3.

Table 1. The Independent Variables of BBD

			levels		
variables	symbol	unit	lowest (−1)	central (0)	highest (+1)
concentration of sodium cholate	*A*	%	1.5	2.5	3.5
concentration of PLGA	*B*	mg/mL	15	20	25
ratio of oil−water	*C*	%	30	50	70

Table 2. The Dependent Variables of BBD

variables	unit	symbol	constraints
size of nanoparticles	nm	Y_1	minimize
PDI of nanoparticles		Y_2	minimize
encapsulation efficiency of CUR	%	Y_3	maximize
encapsulation efficiency of PTX	%	Y_4	maximize
total encapsulation efficiency	%	Y_5	maximize

Variance analysis (ANOVA) was used to verify the polynomial equation generated after analysis, and the relationship between all variables and their influence on the response were predicted. Subsequently, the contour maps (2D) and response surface maps (3D) were generated by the software to understand the relationships between variables and their interactions.

2.3. Characterization of PLGA-CUR-PTX Nanoparticles. *2.3.1. Nanoparticle Size and PDI Measurements.* The PLGA-CUR-PTX nanoparticle (0.02 mL) suspension was diluted with pure water (2 mL), and the size and PDI of the PLGA-CUR-PTX nanoparticles were measured by dynamic light scattering (DLS) using a nanozetasizer (Nano-ZS90, Malvern, UK). Each result was measured in triplicate.

2.3.2. Drug Encapsulation Efficiency (EE) Measurements. After freeze-drying, a certain amount of PLGA-CUR-PTX nanoparticles was dissolved in 50% acetonitrile aqueous solution containing 0.05% phosphoric acid to extract CUR and PTX. The concentration of drugs in the PLGA-CUR-PTX nanoparticles was then determined by high-performance liquid chromatography (HPLC, Agilent, USA) with the following conditions: Keromasil 100-5-C18 (4.6 × 150 nm) chromatographic column; mobile phase: 0.1% phosphoric acid aqueous solution and acetonitrile (50:50, v/v); flow rate of 1 mL/min; detection wavelength of 227 nm; column temperature of 30 ± 0.1 °C; injection volume of 20 μL. The drug EE was calculated by the following equations, and each result was measured in triplicate:

$$\text{EE of CUR (\%)} = \frac{\text{weight of the encapsulated drug of CUR}}{\text{total weight of CUR}} \times 100\%$$

$$\text{EE of PTX (\%)} = \frac{\text{weight of the encapsulated drug of PTX}}{\text{total weight of PTX}} \times 100\%$$

$$\text{total EE (\%)} = \frac{\text{weight of the total encapsulated drug}}{\text{total weight of the total drug}} \times 100\%$$

$$\text{drug loading efficiency (\%) (LE)} = \frac{\text{EE\%} \times \text{weight of the drug}}{\text{weight of PLGA}}$$

2.3.3. Morphological Characterization of PLGA-CUR-PTX Nanoparticles. The shape and surface morphology of the optimized PLGA-CUR-PTX nanoparticles were examined using transmission electronic microscopy (TEM, HT7820, Hitachi, Japan). Briefly, a drop of nanoparticles was spread on a 200-mesh copper grid and dried at room temperature. Then, the sample was negatively stained by adding 1% phosphotungstic acid to the grid. The samples were examined by TEM.

2.3.4. In Vitro Drug Release Study. The *in vitro* release of CUR and PTX from the optimal formulation of PLGA-CUR-PTX nanoparticles was performed in phosphate-buffered saline (PBS) containing 10% ethanol and 0.5% Tween 80, using a membrane diffusion technique.[28] Briefly, 1 mL of the freshly prepared nanoparticle solution corresponding to 636 μg of CUR and 374 μg of PTX was placed in a dialysis bag. Then, the dialysis bags were soaked into 50 mL of PBS containing 10% ethanol and 0.5% Tween 80 as the release media in brown bottles. The brown bottles were kept in an orbital shaker (MAXQ4000, Thermo, USA) at 37 °C and 100 rpm. At predetermined time points (1, 2, 4, 8, 12, 24, 48, 72, and 96 h), a 1 mL sample of release media was withdrawn and replaced with fresh media of an equal volume. The quantitative analysis of CUR and PTX in the release media was detected using the HPLC method. The cumulative drug release percentage was calculated, and the time−drug curve was plotted. The release experiments were performed in triplicate.

Drug release data were fitted into mathematical models of zero-order, first-order, Higuchi, and Korsmeyer−Peppas using the DD solver, an add-in of MS Excel, to build regression analysis of the mathematical expressions to explain the mechanism of drug release.[29−31]

https://doi.org/10.1021/acsomega.2c06359
ACS Omega 2023, 8, 976−986

Table 3. Experimental Arrangement and Results[a]

	independent variables			dependent variables				
formula	A	B	C	Y_1/nm	Y_2	Y_3/%	Y_4/%	Y_5/%
F1	+1	−1	0	76.89 ± 0.59	0.133 ± 0.002	30.07 ± 2.71	70.53 ± 3.59	43.55 ± 0.67
F2	0	+1	−1	112.07 ± 2.16	0.124 ± 0.003	27.22 ± 7.78	58.23 ± 8.31	37.56 ± 6.10
F3	−1	−1	0	110.13 ± 1.86	0.105 ± 0.009	50.22 ± 6.62	70.52 ± 5.15	56.99 ± 2.92
F4	0	0	0	82.81 ± 6.13	0.111 ± 0.006	46.38 ± 7.03	67.82 ± 3.15	53.53 ± 4.08
F5	0	+1	+1	119.13 ± 1.15	0.098 ± 0.004	50.82 ± 8.03	66.99 ± 0.99	56.21 ± 5.16
F6	+1	0	+1	81.72 ± 0.68	0.093 ± 0.013	41.93 ± 4.32	66.65 ± 4.08	50.17 ± 1.95
F7	+1	+1	0	96.24 ± 1.26	0.104 ± 0.020	34.11 ± 4.34	62.30 ± 3.69	43.50 ± 3.95
F8	0	−1	+1	82.53 ± 1.37	0.131 ± 0.003	45.55 ± 7.17	73.44 ± 4.50	54.85 ± 4.33
F9	0	−1	−1	92.9 ± 1.22	0.150 ± 0.026	23.07 ± 5.68	65.42 ± 2.00	37.18 ± 3.57
F10	−1	0	+1	92.48 ± 1.33	0.133 ± 0.016	58.03 ± 7.11	78.36 ± 2.66	64.80 ± 5.30
F11	−1	0	−1	87.54 ± 0.27	0.129 ± 0.019	53.45 ± 9.37	71.29 ± 3.21	59.40 ± 5.22
F12	0	0	0	91.63 ± 1.94	0.246 ± 0.007	38.15 ± 8.11	68.33 ± 4.46	48.21 ± 4.09
F13	0	0	0	108.13 ± 0.70	0.122 ± 0.014	47.97 ± 8.00	78.57 ± 4.37	58.17 ± 3.88
F14	−1	1	0	85.04 ± 1.94	0.117 ± 0.025	48.75 ± 10.50	72.66 ± 4.05	56.72 ± 6.29
F15	+1	0	−1	112.03 ± 0.84	0.128 ± 0.027	15.19 ± 5.40	60.37 ± 8.22	30.25 ± 2.14

[a]Notes: A, concentration of sodium cholate; B, concentration of PLGA; C, ratio of oil−water; Y_1, size of nanoparticles (nm); Y_2, PDI of nanoparticles; Y_3, EE of CUR (%); Y_4, EE of PTX (%); Y_5, total EE (%). Responses are expressed as the mean ± SD (n = 3).

2.3.5. In Vitro Antitumor Efficacy. The cytotoxicity of PLGA-CUR-PTX nanoparticles was determined in 4T1 by the MTT method. Briefly, the breast cancer cell line 4T1 was maintained in DMEM supplemented with 10% (v/v) FBS, 100 U/mL penicillin, and 100 μg/mL streptomycin and grown in a humidified incubator at 37 °C and 5% CO_2. 4T1 cells were seeded in 96-well microplates with a density of 3×10^3 cells/well and incubated for 24 h. Cells were exposed concomitantly to PLGA-CUR-PTX nanoparticles (300 μg/mL) and the relative concentrations of free CUR (7.62 μg/mL), free PTX (4.83 μg/mL), and free CUR (7.62 μg/mL) + free PTX (4.83 μg/mL). The control group without drug addition was used as a negative control. Wells containing only drugs without cells were used as the blank group. After 48 h, the original culture medium was discarded, and the cells were washed twice with PBS. A solution of 100 μL of MTT (0.5 mg/mL) diluted with base medium was added to each well and incubated for 4 h. Then, the optical density (OD) values were measured at 490 nm using a microplate reader (Varioskan LUX, Thermo, USA). Cell viability was calculated according to the following formula: cell viability (%) = $(OD_{groups} - OD_{blank})/(OD_{control} - OD_{blank}) \times 100\%$. Six parallel experiments were performed in each group. Furthermore, 4T1 cells were exposed with the blank PLGA nanoparticles without drugs in different concentrations (0−500 μg/mL) for 24 h to assess the biocompatibility of the carriers.

To determine the half maximal inhibitory concentration (IC_{50}) for 4T1 and MCF-7 cells for 48 h, the same method was repeated using different concentrations of PLGA-CUR-PTX nanoparticles, CUR, PTX, and CUR+PTX. GraphPad Prism version 8 (GraphPad Software, San Diego, CA, USA) was used to analyze the results. To further investigate the synergistic effect of CUR and PTX, the combination index (CI) of the two drugs was calculated using the equation[32] $CI = H/H_1 + D/D_1$, where H_1 and D_1 are the concentrations of CUR and PTX alone that kill 50% of the cell population and H and D are the concentrations of CUR and PTX in nanoparticles that give similar cell killing efficacy (50%) in combination. Values of CI at <1, =1, and >1 represent synergistic, additive, and antagonistic effects, respectively.

3. RESULTS AND DISCUSSION

3.1. Preparation of PLGA-CUR-PTX Nanoparticles. A single emulsion solvent evaporation method was used to

Table 4. The ANOVA Results for All Responses[a]

responses	sum of squares	df	mean square	F value	P value	
Y_1	1528.13	9	169.79	0.83	0.6185	not significant
Y_2	0.01	9	0.00	0.29	0.9478	not significant
Y_3	2000.78	9	222.31	8.14	0.0163	significant
Y_4	379.80	9	42.20	2.09	0.2159	not significant
Y_5	1236.67	9	137.41	6.74	0.0245	significant

[a]Notes: Y_1, size of nanoparticles (nm); Y_2, PDI of nanoparticles; Y_3, EE of CUR (%); Y_4, EE of PTX (%); Y_5, total EE (%).

Table 5. ANOVA for the Surface Quadratic Model for the EE of CUR (Y_3)[a]

source	sum of squares	df	mean square	F value	P value
model	2000.78	9	222.31	8.14	0.0163
A	993.78	1	993.78	36.40	0.0018
B	18.00	1	18.00	0.66	0.4536
C	748.77	1	748.77	27.43	0.0033
AB	7.58	1	7.58	0.28	0.6207
AC	122.71	1	122.71	4.49	0.0874
BC	0.32	1	0.32	0.01	0.9180
A^2	4.09	1	4.09	0.15	0.7145
B^2	72.54	1	72.54	2.66	0.1640
C^2	34.81	1	34.81	1.27	0.3100
residual	136.51	5	27.30	NA	NA
lack of fit	80.98	3	26.99	0.97	0.5431
pure error	55.53	2	27.77	NA	NA
cor total	2137.31	14	NA	NA	NA

[a]Notes: A, concentration of sodium cholate; B, concentration of PLGA; C, ratio of oil−water; Y_1, size of nanoparticles (nm); Y_2, PDI of nanoparticles.

https://doi.org/10.1021/acsomega.2c06359
ACS Omega 2023, 8, 976−986

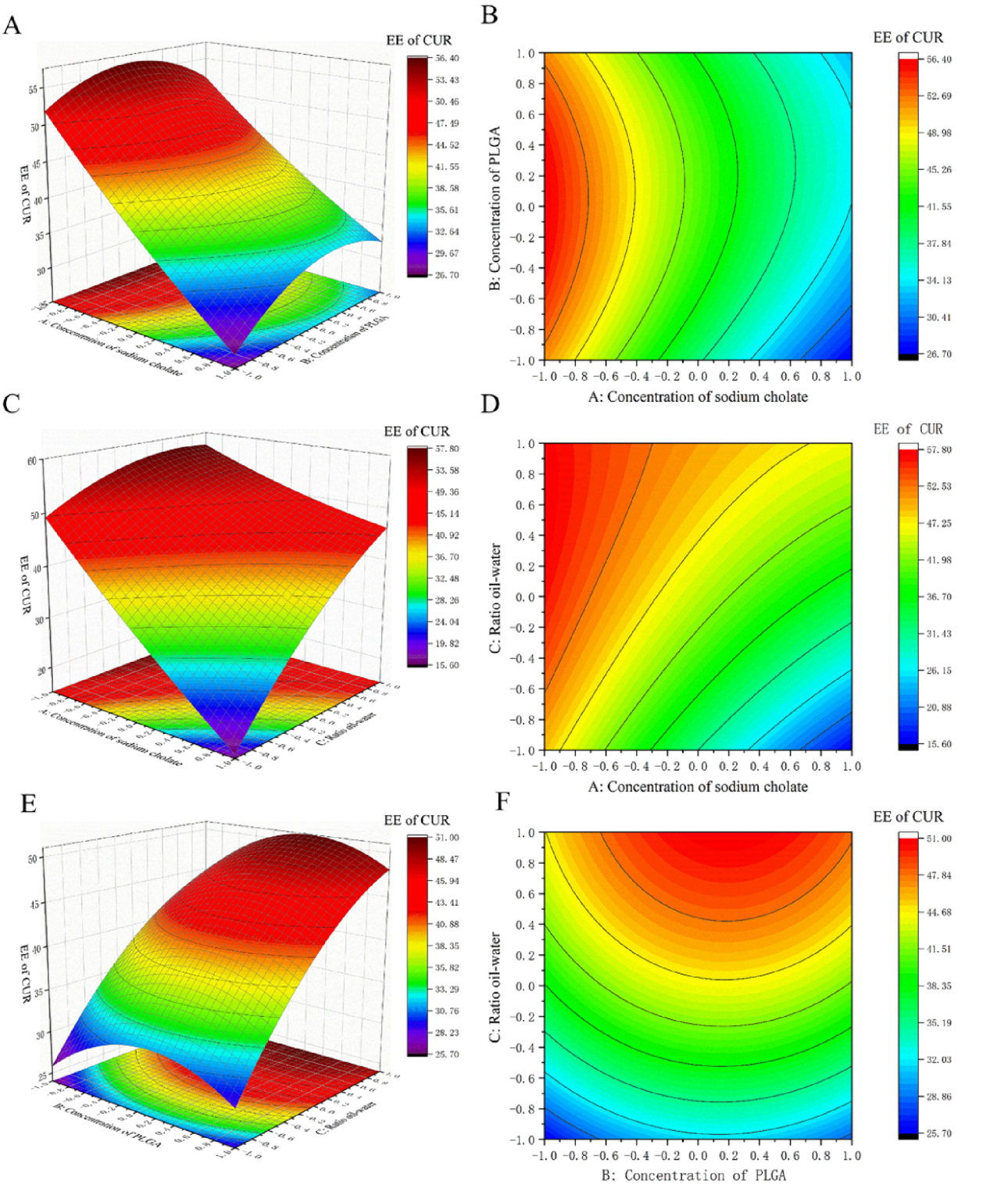

Figure 1. 3D response surface plots and 2D contour map for PLGA-CUR-PTX nanoparticles showing the effect of (A,B) concentration of sodium cholate and concentration of PLGA, (C,D) concentration of sodium cholate and the ratio of oil−water, and (E,F) concentration of PLGA and the ratio of oil−water on the EE of CUR.

fabricate CUR and PTX coloaded PLGA nanoparticles. The organic mixture of PLGA, CUR, and PTX was emulsified with the aqueous phase containing sodium cholate by sonication. Finally, the PLGA-CUR-PTX nanoparticles were purified by ultrafiltration. A Box−Behnken design (BBD) of 15 runs, three factors at three levels (3^3), with three replicates at the center point, was constructed to study the influence of different factor variables on the size, PDI, and EE of PLGA-CUR-PTX nanoparticles. The experimental results concerning the size of the nanoparticles, PDI of the nanoparticles, and EE from all experiments are given in Table 3.

3.2. Optimization of PLGA-CUR-PTX Nanoparticles. *3.2.1. Particle Size and PDI.* The particle size ranged from 76.89 ± 0.59 to 119.13 ± 1.15 nm, and the mean PDI values

https://doi.org/10.1021/acsomega.2c06359
ACS Omega 2023, 8, 976−986

Table 6. ANOVA for the Quadratic Model for the Total EE (Y_5)[a]

source	sum of squares	df	mean square	F value	P value
model	1236.67	9	137.41	6.74	0.0245
A	620.08	1	620.08	30.40	0.0027
B	0.2527	1	0.25	0.012	0.9157
C	474.90	1	474.90	23.28	0.0048
AB	0.0116	1	0.01	0.00	0.9819
AC	52.62	1	52.62	2.58	0.1691
BC	0.25	1	0.25	0.01	0.9166
A^2	2.35	1	2.35	0.12	0.7481
B^2	56.40	1	56.40	2.77	0.1572
C^2	32.02	1	32.01	1.57	0.2656
residual	101.98	5	20.40	NA	NA
lack of fit	52.31	3	17.44	0.70	0.6325
pure error	49.66	2	24.83	NA	NA
cor total	1338.65	14	NA	NA	NA

[a]Notes: A, concentration of sodium cholate; B, concentration of PLGA; C, ratio of oil−water; Y_1, size of nanoparticles (nm); Y_2, PDI of nanoparticles.

were all less than 0.25, demonstrating the good uniformity of the prepared nanoparticles (Table 3). It is well-recognized that the suitable size of nanoparticles for antitumor therapy is less than 200 nm.[33] Thus, the size of all prepared nanoparticles was beneficial to their application in antitumor therapy.

The function to predict the studied process variables affecting the size of nanoparticles (Y_1) was automatically generated by Design Expert software:

$$Y_1 = 92.92 - 1.08A + 6.25B - 3.54C + 11.11AB - 8.9AC + 4.36BC - 4.48A^2 + 3.65B^2 + 5.1C^2 \ (R^2 = 0.6257)$$

The function to predict the studied process variables affecting the PDI of nanoparticles (Y_2) was automatically generated by Design Expert software:

$$Y_2 = 0.19 - 0.003A - 0.009B - 0.009C - 0.01AB - 0.009AC - 0.001BC - 0.038A^2 - 0.034B^2 - 0.028C^2 \ (R^2 = 0.5632)$$

The results of the ANOVA (Table 4) showed that P for the model was higher than 0.05 for Y_1 (size of nanoparticles) and Y_2 (PDI of nanoparticles), indicating that the size of nanoparticles and the PDI of nanoparticle variation were not influenced by any of the factors studied.

3.2.2. EE of Drugs. BBD was performed to determine the effects of the concentration of sodium cholate, the concentration of PLGA, and the ratio of oil−water on the total EE and on the EE of CUR and PTX for the optimization of nanoparticle preparation. The results of all experiments are listed in Table 3.

3.2.2.1. EE of CUR. The EE of CUR ranged from 15.19 ± 5.40 to 58.03 ± 7.01% (Table 3). The function to predict the studied process variables affecting the EE of CUR (Y_3) was automatically generated by Design Expert software:

$$Y_3 = 44.17 - 11.15A + 1.50B + 9.67C + 1.38AB + 5.54AC + 0.28BC + 1.05A^2 - 4.43B^2 - 3.07C^2 \ (R^2 = 0.9361)$$

The R^2 (coefficient of determination) value of the model was 0.9361. Meanwhile, the lack of fit was not significant (P = 0.5431). These values confirmed that the model was adequate for predicting the EE under any combination of values of the variables inside the experimental domain. From the equation, a positive value indicated a synergistic effect in the regression model; on the contrary, a negative value indicated an antagonistic effect.[34] Factors B, C, AB, AC, BC, and A^2 had a positive effect on response Y_3, and A, B^2, and C^2 had a negative effect on the response Y_3. Analysis of data by ANOVA of the proposed model indicated the significant effect of all factors on Y_3 (EE of CUR) (P = 0.0163). According to the results of the statistical analysis (Tables 4 and 5), it was found that two independent process variables, namely, the concentration of sodium cholate (A) and the ratio of oil−water (C), had significant effects on the EE of CUR ($P < 0.05$), while another variable, the concentration of PLGA (B), had no independent impact on the EE of CUR ($P > 0.05$).

Figure 1 shows the influences of the concentration of sodium cholate, the ratio of oil−water, and the concentration of PLGA on the response variable. It clearly exhibits the response surface plots (3D) and contour plots (2D) (Figure 1), where an obvious decrease in the EE of CUR was observed with an increase in the concentration of sodium cholate from a low level to a high level with a constant ratio of oil−water. This phenomenon was similar to previous studies.[35−39] This may be because sodium cholate is a surfactant with a high HLB value (HLB = 18), which usually leads to a low EE.[40] On the other hand, the increase in the sodium cholate concentration can improve the solubility of hydrophobic drugs in aqueous solution and reduce the interfacial tension of the emulsion. As a result, a high concentration of sodium cholate will reduce the interfacial tension, promoting the release of drugs into the external water phase during mixing, leaving fewer drugs in the emulsion droplets and resulting in a decreased EE.[39,41,42] Furthermore, an obvious increase in the EE of CUR was observed with an increase in the ratio of oil−water from a low level to a high level with a constant concentration of sodium cholate (Figure 1). This may be because increasing the ratio of the organic phase increases the viscosity of the emulsion and slows drug diffusion in the aqueous phase, thus increasing the EE of CUR.

3.2.2.2. EE of PTX. The EE of PTX ranged from 58.23 ± 8.31 to 78.57 ± 4.31% (Table 3). The function to predict the studied process variables affecting the EE of PTX (Y_4) was automatically generated by Design Expert software:

$$Y_4 = 71.57 - 4.12A - 2.47B + 3.77C - 2.59AB - 0.20AC + 0.18BC + 0.29A^2 - 2.86B^2 - 2.69C^2 \ (R^2 = 0.7899)$$

The results of the ANOVA test (Table 4) showed that P for the model was higher than 0.05 for Y_4 (EE of PTX), indicating that the EE of PTX was not influenced by any of the factors studied.

3.2.2.3. Total EE. The total EE ranged from 30.25 ± 2.14 to 64.80 ± 5.30% (Table 3). The function to predict the studied process variables affecting the total EE (Y_5) was automatically generated by Design Expert software:

$Y_5 = 53.30 - 8.80A + 0.18B + 7.70C + 0.05AB + 3.63AC + 0.25BC + 0.80A^2 - 3.9B^2 - 2.94C^2$ ($R^2 = 0.9238$)

Analysis of data by ANOVA of the proposed model indicated a significant effect of all factors on Y_5 (total EE), with a P value of 0.0246. The R^2 value of the model was 0.9238. Meanwhile, the lack of fit was not significant (P = 0.6326). These values confirmed that the model was adequate for predicting the EE under any combination of values of the variables inside the experimental domain. Factors B, C, AB, AC, BC, and A^2 had a positive effect on the response Y_5, and A, B^2,

https://doi.org/10.1021/acsomega.2c06359
ACS Omega 2023, 8, 976−986

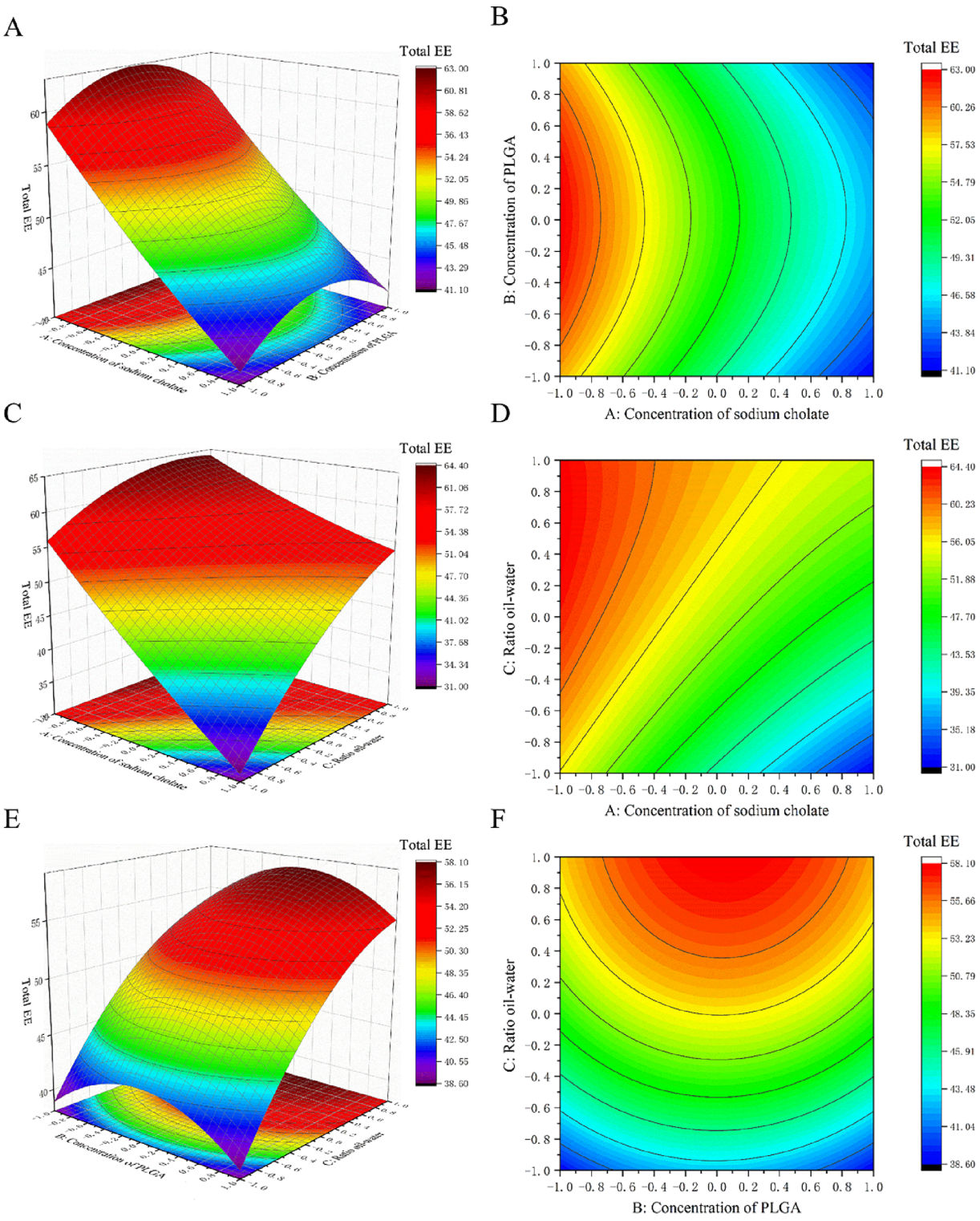

Figure 2. 3D response surface plots and 2D contour map for PLGA-CUR-PTX nanoparticles showing the effect of (A,B) concentration of sodium cholate and concentration of PLGA, (C,D) concentration of sodium cholate and the ratio of oil−water, and (E,F) concentration of PLGA and the ratio of oil−water on the total EE.

and C^2 had a negative effect on the response Y_5. According to the results of the statistical analysis (Tables 4 and 6), it was found that two independent process variables, namely, the concentration of sodium cholate (A) and the ratio of oil−water (C), had significant effects on the total EE ($P < 0.05$), while another variable, the concentration of PLGA (B), had no independent impact on the total EE ($P > 0.05$).

The total EE was significantly affected by both the sodium cholate concentration and the ratio of oil−water, with a higher concentration of sodium cholate leading to a lower total EE and conversely a higher oil−water ratio leading to a higher total EE (Figure 2). The effects of the surfactant concentration and the ratio of oil−water on the total EE were similar to their effect on the EE of CUR, which was probably due to the fact

https://doi.org/10.1021/acsomega.2c06359
ACS Omega 2023, 8, 976−986

Table 7. The Predicted Values and the Optimized Response Values Observed for PLGA-CUR-PTX Nanoparticles[a]

responses	predicted values	observation values
Y_1	95.53 nm	99.94 nm
Y_2	0.139	0.101
Y_3	57.76%	63.53%
Y_4	78.57%	80.64%
Y_5	64.80%	69.24%

[a]Notes: Y_1, size of nanoparticles (nm); Y_2, PDI of nanoparticles; Y_3, EE of CUR (%); Y_4, EE of PTX (%); Y_5, total encapsulation efficiency (%).

that the EE of the other drug PTX is not affected by any experimental factor. So, the change in the total EE is mainly caused by the change in the EE of CUR.

3.2.3. Optimal Formulation for PLGA-CUR-PTX Nanoparticles. Optimization was performed by employing the desirability method upon application of constraints to the three independent variables (*A*, concentration of sodium cholate; *B*, concentration of PLGA; *C*, ratio of oil−water). To obtain the maximum EE of the PLGA-CUR-PTX nanoparticles, software was used to determine the levels of the three independent variables. The levels of *A*, *B*, and *C* were found to be 1.5% w/v, 20.18 mg/mL, and 70% v/v, respectively. The predicted values are listed in Table 7. The optimized PLGA-CUR-PTX nanoparticles have a desirability of 0.990. The predicted levels of each variable will be used to prepare the optimized PLGA-CUR-PTX nanoparticles to confirm the prediction. The optimized response values of PLGA-CUR-PTX nanoparticles are shown in Table 7. The optimal size was 99.94 nm, the PDI was 0.101, and the optimal EE values were 63.53 (LE: 2.54%), 80.64 (LE: 1.61%), and 69.24% (LE: 4.15%) for CUR, PTX, and total drugs, respectively. This size was suitable for antitumor therapy because the optimized nanoparticles could passively target the tumor site due to the EPR effects.[43] The narrow size distribution of nanoparticles indicated by a lower PDI can contribute to the high reproducibility of experiments and results. The high EE of the optimized nanoparticles can avoid the waste of drugs during the formulation process.

3.3. Characterization of Optimized PLGA-CUR-PTX Nanoparticles. *3.3.1. Size Distribution and Morphological Characterization of Optimal PLGA-CUR-PTX Nanoparticles.* As shown in Figure 3A and Table 7, the size and PDI of the optimized nanoparticles were measured to be around 100 nm and 0.1, respectively, indicating a uniform size distribution.

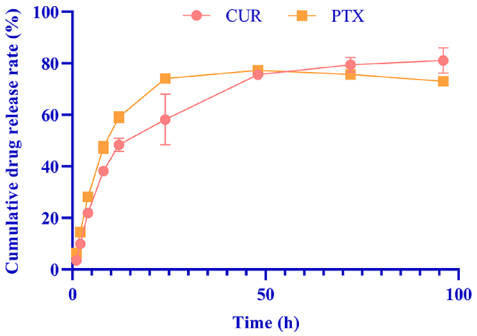

Figure 4. *In vitro* drug release study of the optimized PLGA-CUR-PTX nanoparticles at pH 7.4 (each group represents n = 3, mean ± standard deviation).

Table 8. Release Kinetics Parameters of *In Vitro* CUR and PTX Release from PLGA-CUR-PTX Nanoparticles

	the release equations		model coefficient (R^2)	
kinetics model	CUR	PTX	CUR	PTX
zero-order	$M_t/M_\infty = 1.116 \times t$	$M_t/M_\infty = 1.096 \times t$	0.3535	−0.3298
first-order	$M_t/M_\infty = F = 100 \times [1 - \exp(-0.038 \times t)]$	$M_t/M_\infty = F = 100 \times [1 - \exp(-0.065 \times t)]$	0.8759	0.7237
Higuchi	$M_t/M_\infty = F = 9.795 \times t^{1/2}$	$M_t/M_\infty = F = 10.035 \times t^{1/2}$	0.8907	0.6076
Korsmeyer−Peppas	$M_t/M_\infty = F = 14.994 \times t^{0.392}$	$M_t/M_\infty = F = 22.105 \times t^{0.229}$	0.9299	0.8131

3.3.2. In Vitro Drug Release Study. The release profile of CUR and PTX from optimized PLGA-CUR-PTX nanoparticles at pH 7.4 is shown in Figure 4. The drug release profile from nanoparticles showed a biphasic release behavior, which consisted of an initial burst release (the cumulative drug release rates of CUR and PTX during the burst release period were 48.5 ± 2.57 and 59.1 ± 2.14%, respectively) within 12 h

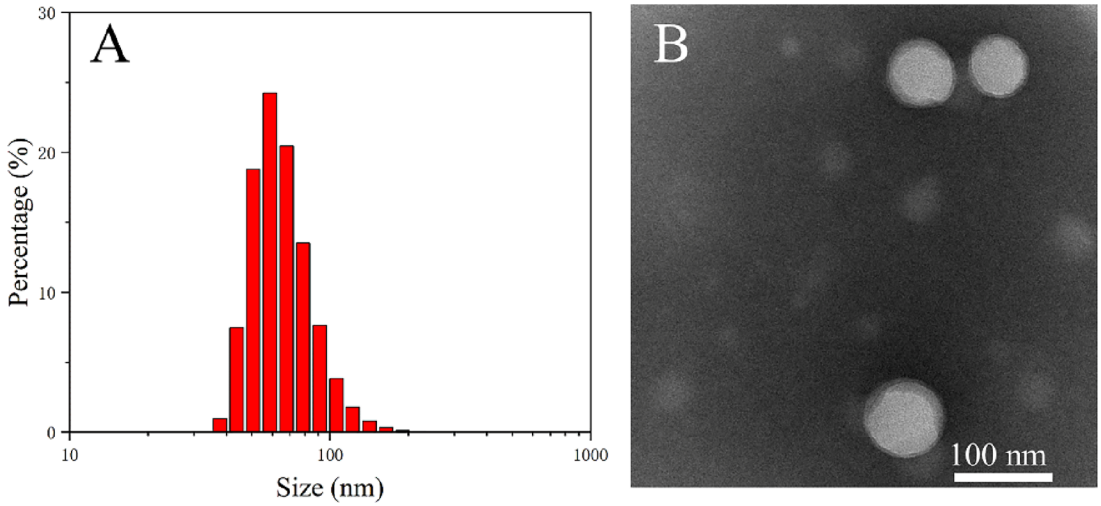

Figure 3. (A) Size distribution and (B) TEM image of optimized PLGA-CUR-PTX nanoparticles. TEM scale bar: 100 nm.

https://doi.org/10.1021/acsomega.2c06359
ACS Omega 2023, 8, 976−986

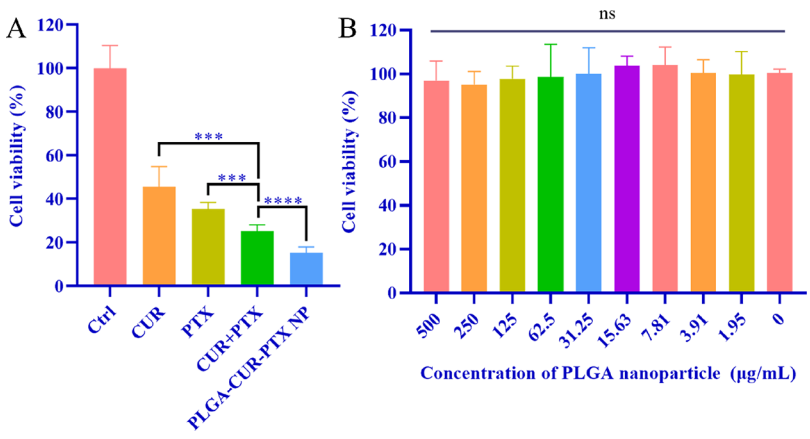

Figure 5. *In vitro* antitumor efficacy. (A) Cell viability of 4T1 breast cancer cells incubated with different treatments for 48 h. (B) Cell viability of 4T1 breast cancer cells incubated with different concentrations of blank PLGA nanoparticles for 24 h. Each group represents $n = 6$, mean ± standard deviation, ***$P < 0.01$, ****$P < 0.001$, ns: no significance.

Table 9. IC_{50} Values for Different Drugs and Formulations on 4T1 and MCF-7 Cells after 48 h of Incubation

	4T1 IC_{50}(ng/mL)			MCF-7 IC_{50} (ng/mL)		
drugs	CUR	PTX	CI_{50}	CUR	PTX	CI_{50}
CUR	13,868			10,338		
PTX		420.7			313.8	
CUR+PTX	275.1	148.5	0.37	180.9	97.86	0.33
PLGA-CUR-PTX nanoparticles	123.7	66.7	0.17	109.9	59.37	0.20

followed by controlled release in the subsequent time (the cumulative drug release rates of CUR and PTX during the controlled release period were 81.1 ± 4.97 and 73.0 ± 1.34%, respectively). The initial burst release from PLGA-CUR-PTX nanoparticles was attributed to the immediate desorption of drug molecules adsorbed onto the particle surface, and a shorter average diffusion path due to the nanoscale nanoparticles led to rapid drug molecule release.[44] Thereafter, the slower release during the controlled release period was due to drug molecules resolved into the release medium from the nanoparticle core through interconnected pores and channels in the polymeric matrix.[45]

The drug release mechanism was analyzed by different mathematical models (Table 8). Compared with the zero-order, first-order, and Higuchi models, the Korsmeyer–Peppas model was the best fit for the release behavior of CUR and PTX, with R^2 values of 0.9299 and 0.8131, respectively. Based on the diffusional exponent $n < 0.5$, the release mechanisms of CUR ($n = 0.392$) and PTX ($n = 0.229$) were diffusion and fundamentally quasi-Fickian diffusion.[46]

3.4. *In Vitro* Antitumor Efficacy. The *in vitro* antitumor efficacy of PLGA-CUR-PTX nanoparticles, free CUR, free PTX, and free CUR combined with free PTX in 4T1 breast cancer cells was assessed by the MTT assay (Figure 5A). The 4T1 cells were treated with different treatment groups for 48 h, and the cell activity of all groups was significantly lower than that of the control group. The cell activity of the free CUR combined with free PTX group was significantly lower than that of the free CUR group ($P < 0.001$) and the free PTX group ($P < 0.001$); moreover, the PLGA-CUR-PTX nanoparticle group further inhibited the 4T1 cell activity ($P < 0.0001$). As shown in Figure 5B, the cell viability was nearly 100% after incubation with nanoparticles in the concentration range of 0 to 500 μg/mL, demonstrating that the PLGA-CUR-PTX nanoparticles had superior biocompatibility.

The therapeutic efficacy of the drug was further investigated by measuring the IC_{50} of CUR, PTX, CUR+PTX, and PLGA-CUR-PTX nanoparticles on 4T1 and MCF-7 cells (Table 9). The CI values of CUR+PTX were 0.37 on 4T1 cells and 0.33 on MCF-7 cells. Moreover, the CI values were even lower for PLGA-CUR-PTX nanoparticles, with 0.17 on 4T1 cells and 0.20 on MCF-7 cells, which demonstrated the good synergistic antitumor effect of CUR and PTX. Moreover, CUR and PTX coloaded PLGA nanoparticles had the lowest IC_{50} values on 4T1 (CUR: 123.7 ng/mL; PTX: 66.7 ng/mL) and MCF-7 (CUR: 109.9 ng/mL; PTX: 59.37 ng/mL) cells, which were similar with the previous report.[47] In this study, CUR combined with PTX could decline the IC_{50} of both CUR and PTX. These results demonstrated that coloading CUR and PTX in PLGA nanoparticles can improve the therapeutic effects and bioavailability of CUR and PTX.

4. CONCLUSIONS

In this study, Box–Behnken design (BBD) was used to develop and optimize CUR and PTX coloaded PLGA nanoparticles. The influence of the surfactant concentration, PLGA concentration, and the ratio of oil–water on the size, polydispersity index (PDI), and drug encapsulation efficiency were clarified, and the optimum conditions were obtained through the predictive mathematical model, in which the surfactant concentration was 1.5% w/v, the PLGA concentration was 20.18 mg/mL, and the ratio of oil–water was 70% v/v. Under this optimal condition, PLGA-CUR-PTX nanoparticles were successfully produced with a small particle size (99.94 nm) and PDI (0.101) and a high encapsulation efficiency for both CUR (63.53%) and PTX (80.64%). Coloading of CUR and PTX into PLGA nanoparticles could increase the solubility of CUR and PTX in physicochemical conditions and prolong the drug release rate. The optimized PLGA-CUR-PTX nanoparticles produced enhanced cytotoxicity with reduced IC_{50} values on 4T1 and MCF-7 breast cancer cells compared with the free drug combination group. Thus, the developed PLGA-CUR-PTX nanoparticles hold potential as an alternative to existing tumor chemotherapies.

https://doi.org/10.1021/acsomega.2c06359
ACS Omega 2023, 8, 976–986

AUTHOR INFORMATION

Corresponding Authors

Wenjun Zou − *Department of Chinese Materia Medica, School of Pharmacy, Chengdu University of Traditional Chinese Medicine, Chengdu, Sichuan 610075, China*; Email: zouwenjun@163.com

Jianming Wu − *Sichuan Key Medical Laboratory of New Drug Discovery and Druggability Evaluation, Luzhou Key Laboratory of Activity Screening and Druggability Evaluation for Chinese Materia Medica, School of Pharmacy and School of Basic Medical Sciences, Southwest Medical University, Luzhou 646000, China*; Email: jianmingwu@swmu.edu.cn

Qingze Fan − *Department of Pharmacy, The Affiliated Hospital of Southwest Medical University, Luzhou, Sichuan 646099, China; Sichuan Key Medical Laboratory of New Drug Discovery and Druggability Evaluation, Luzhou Key Laboratory of Activity Screening and Druggability Evaluation for Chinese Materia Medica, School of Pharmacy, Southwest Medical University, Luzhou 646000, China*; orcid.org/0000-0002-3212-0002; Email: qingzefan017@swmu.edu.cn

Authors

Haiyang Hu − *Department of Chinese Materia Medica, School of Pharmacy, Chengdu University of Traditional Chinese Medicine, Chengdu, Sichuan 610075, China; Sichuan Key Medical Laboratory of New Drug Discovery and Druggability Evaluation, Luzhou Key Laboratory of Activity Screening and Druggability Evaluation for Chinese Materia Medica, School of Pharmacy, Southwest Medical University, Luzhou 646000, China*

Zuyue Liao − *Department of Pharmacy, The Affiliated Hospital of Southwest Medical University, Luzhou, Sichuan 646099, China*

Mengyao Xu − *Department of Pharmacy, The Affiliated Hospital of Southwest Medical University, Luzhou, Sichuan 646099, China*

Shengli Wan − *Department of Pharmacy, The Affiliated Hospital of Southwest Medical University, Luzhou, Sichuan 646099, China; Sichuan Key Medical Laboratory of New Drug Discovery and Druggability Evaluation, Luzhou Key Laboratory of Activity Screening and Druggability Evaluation for Chinese Materia Medica, School of Pharmacy, Southwest Medical University, Luzhou 646000, China*

Yuesong Wu − *Department of Pharmacy, The Affiliated Hospital of Southwest Medical University, Luzhou, Sichuan 646099, China; Sichuan Key Medical Laboratory of New Drug Discovery and Druggability Evaluation, Luzhou Key Laboratory of Activity Screening and Druggability Evaluation for Chinese Materia Medica, School of Pharmacy, Southwest Medical University, Luzhou 646000, China*

Complete contact information is available at: https://pubs.acs.org/10.1021/acsomega.2c06359

Author Contributions

⊥H.H. and Z.L. contributed equally to this work.

Notes

The authors declare no competing financial interest.

ACKNOWLEDGMENTS

This study was supported by The Science and Technology Planning Project of Sichuan Province, China (nos. 2022NSFSC1429 and 2022JDJQ0061), The National Natural Science Foundation of China (no. 22208269), The Joint Project between Luzhou Municipal People's Government and Southwest Medical University (no. 2021LZXNYD-J17), and the Foundation of Southwest Medical University (no. 2021ZKZD012).

REFERENCES

(1) Sung, H.; Ferlay, J.; Siegel, R. L.; Laversanne, M.; Soerjomataram, I.; Jemal, A.; Bray, F. Global Cancer Statistics 2020: Glonocan Estimates of Incidence and Mortality Worldwide for 36 Cancers in 185 Countrie. *Ca-Cancer J. Clin.* **2021**, 209−249.

(2) Siegel, R. L.; Miller, K. D.; Fuchs, H. E.; Jemal, A. Cancer statistics, 2022. *Ca-Cancer J. Clin.* **2022**, *72*, 7−33.

(3) Jiang, S.; Mou, Y.; He, H.; Yang, D.; Qin, L.; Zhang, F.; Zhang, P. Preparation and Evaluation of Self-Assembly Soluplus-sodium cholate-phospholipid Ternary Mixed Micelles of Docetaxel. *Drug Dev. Ind. Pharm.* **2019**, *45*, 1788−1798.

(4) Rawal, S.; Patel, M. M. Threatening Cancer with Nanoparticle Aided Combination Oncotherapy. *J. Controlled Release* **2019**, *301*, 76−109.

(5) Abu Samaan, T. M.; Samec, M.; Liskova, A.; Kubatka, P.; Büsselberg, D. Paclitaxel's Mechanistic and Clinical Effects on Breast Cancer. *Biomolecules* **2019**, *9*, 789.

(6) Madani, F.; Esnaashari, S. S.; Bergonzi, M. C.; Webster, T. J.; Younes, H. M.; Khosravani, M.; Adabi, M. Paclitaxel/Methotrexate Co-Loaded PLGA Nanoparticles in Glioblastoma Treatment: Formulation Development and In Vitro Antitumor Activity Evaluation. *Life Sci.* **2020**, *256*, 117943.

(7) Ezhilarasan, D.; Lakshmi, T.; Mallineni, S. K. Nano-based Targeted Drug Delivery for Lung Cancer: Therapeutic Avenues and Challenges. *Nanomedicine* **2022**, DOI: 10.2217/nnm-2021-0364.

(8) Xiang, Y.; Guo, Z.; Zhu, P.; Chen, J.; Huang, Y. Traditional Chinese Medicine as a Cancer Treatment: Modern Perspectives of Ancient but Advanced Science. *Cancer Med.* **2019**, *8*, 1958−1975.

(9) Mujokoro, B.; Madani, F.; Esnaashari, S.; Khosravani, M.; Adabi, M. Combination and Co-Delivery of Methotrexate and Curcumin: Preparation and In Vitro Cytotoxic Investigation on Glioma Cells. *J. Pharm. Innovation* **2020**, *15*, 617−626.

(10) Patra, S.; Pradhan, B.; Nayak, R.; Behera, C.; Rout, L.; Jena, M.; Efferth, T.; Bhutia, S. K. Chemotherapeutic Efficacy of Curcumin and Resveratrol Against Cancer: Chemoprevention, Chemoprotection, Drug Synergism and Clinical Pharmacokinetics. *Semin. Cancer Biol.* **2021**, *73*, 310−320.

(11) Quispe-Soto, E. T.; Calaf, G. M. Effect of Curcumin and Paclitaxel on Breast Carcinogenesis. *Int. J. Oncol.* **2016**, *49*, 2569−2577.

(12) Wicki, A.; Witzigmann, D.; Balasubramanian, V.; Huwyler, J. Nanomedicine in Cancer Therapy: Challenges, Opportunities, and Clinical Applications. *J. Controlled Release* **2015**, *200*, 138−157.

(13) Wang, A. Z.; Langer, R.; Farokhzad, O. C. Nanoparticle Delivery of Cancer Drugs. *Annu. Rev. Med.* **2012**, *63*, 185−198.

(14) Zhang, J.; Wang, N.; Li, Q.; Zhou, Y.; Luan, Y. A Two-Pronged Photodynamic Nanodrug to Prevent Metastasis of Basal-Like Breast Cancer. *Chem. Commun.* **2021**, *57*, 2305−2308.

(15) Zhang, M.; Qin, X.; Xu, W.; Wang, Y.; Song, Y.; Garg, S.; Luan, Y. Engineering of A Dual-Modal Phototherapeutic Nanoplatform for Single NIR Laser-Triggered Tumor Therapy. *J. Colloid Interface Sci.* **2021**, *594*, 493−501.

(16) Zhang, M.; Qin, X.; Zhao, Z.; Du, Q.; Li, Q.; Jiang, Y.; Luan, Y. A Self-Amplifying Nanodrug to Manipulate the Janus-Faced Nature of Ferroptosis for Tumor Therapy. *Nanoscale Horiz.* **2022**, *7*, 198−210.

(17) Parveen, S.; Misra, R.; Sahoo, S. K. Nanoparticles: A Boon to Drug Delivery, Therapeutics, Diagnostics and Imaging. *Nanomedicine* **2012**, *8*, 147−166.

(18) Makadia, H. K.; Siegel, S. J. Poly Lactic-co-Glycolic Acid (PLGA) as Biodegradable Controlled Drug Delivery Carrier. *Polymer* **2011**, *3*, 1377−1397.

(19) Gagliardi, A.; Giuliano, E.; Venkateswararao, E.; Fresta, M.; Bulotta, S.; Awasthi, V.; Cosco, D. Biodegradable Polymeric Nanoparticles for Drug Delivery to Solid Tumors. *Front. Pharmacol.* **2021**, *12*, 601626.
(20) Mora-Huertas, C. E.; Fessi, H.; Elaissari, A. Influence of Process and Formulation Parameters on the Formation of Submicron Particles by Solvent Displacement and Emulsification-Diffusion Methods Critical Comparison. *Adv. Colloid Interface Sci.* **2011**, *163*, 90−122.
(21) Singh, B.; Kumar, R.; Ahuja, N. Optimizing Drug Delivery Systems Using Systematic "Design of Experiments." Part I: Fundamental Aspects. *Crit. Rev. Ther. Drug Carrier Syst.* **2005**, *22*, 27−105.
(22) Du, D.; Zhang, X.; Yu, K.; Song, X.; Shen, Y.; Li, Y.; Wang, F.; Zhifeng, S.; Li, T. Parameter Screening Study for Optimizing the Static Properties of Nanoparticle-Stabilized CO(2) Foam Based on Orthogonal Experimental Design. *ACS Omega* **2020**, *5*, 4014−4023.
(23) Singh, B.; Kapil, R.; Nandi, M.; Ahuja, N. Developing Oral Drug Delivery Systems Using Formulation by Design: Vital Precepts, Retrospect and Prospects. *Expert Opin. Drug Delivery* **2011**, *8*, 1341−1360.
(24) Tavares Luiz, M.; Santos Rosa Viegas, J.; Palma Abriata, J.; Viegas, F.; Testa Moura de Carvalho Vicentini, F.; Lopes Badra Bentley, M. V.; Chorilli, M.; Maldonado Marchetti, J.; Tapia-Blácido, D. R. Design of Experiments (DoE) to Develop and to Optimize Nanoparticles as Drug Delivery Systems. *Eur. J. Pharm. Biopharm.* **2021**, *165*, 127−148.
(25) Bezerra, M. A.; Santelli, R. E.; Oliveira, E. P.; Villar, L. S.; Escaleira, L. A. Response Surface Methodology (RSM) as a Tool for Optimization in Analytical Chemistry. *Talanta* **2008**, *76*, 965−977.
(26) Keskin Gündoğdu, T.; Deniz, İ.; Çalışkan, G.; Şahin, E. S.; Azbar, N. Experimental Design Methods for Bioengineering Applications. *Crit. Rev. Biotechnol.* **2016**, *36*, 368−388.
(27) Shaikh, M. V.; Kala, M.; Nivsarkar, M. Formulation and Optimization of Doxorubicin Loaded Polymeric Nnanoparticles Using Box-Behnken Design: Ex-Vivo Stability and In-Vitro Activity. *Eur. J. Pharm. Sci.* **2017**, *100*, 262−272.
(28) Abouelmagd, S. A.; Sun, B.; Chang, A. C.; Ku, Y. J.; Yeo, Y. Release Kinetics Study of Poorly Water-Soluble Drugs From Nanoparticles: Are We Doing It Right? *Mol. Pharmaceutics* **2015**, *12*, 997−1003.
(29) Dash, S.; Murthy, P. N.; Nath, L.; Chowdhury, P. Kinetic Modeling on Drug Release from Controlled Drug Delivery Systems. *Acta Pol Pharm* **2010**, *67*, 217−223.
(30) Bahari Javan, N.; Rezaie Shirmard, L.; Jafary Omid, N.; Akbari Javar, H.; Rafiee Tehrani, M.; Abedin Dorkoosh, F. Preparation, Statistical Optimisation and In Vitro Characterisation of Poly (3-Hydroxybutyrate-co-3-Hydroxyvalerate)/Poly (Lactic-co-Glycolic Acid) Blend Nanoparticles for Prolonged Delivery of Teriparatide. *J. Microencapsulation* **2016**, *33*, 460−474.
(31) Zhang, Y.; Huo, M.; Zhou, J.; Zou, A.; Li, W.; Yao, C.; Xie, S. DDSolver: An Add-In Program for Modeling and Comparison of Drug Dissolution Profiles. *AAPS J.* **2010**, *12*, 263−271.
(32) Chou, T. C.; Talalay, P. Quantitative Analysis of Dose-Effect Relationships: The Combined Effects of Multiple Drugs or Enzyme Inhibitors. *Adv. Enzyme Regul.* **1984**, *22*, 27−55.
(33) Wang, J.; Sui, M.; Fan, W. Nanoparticles for Tumor Targeted Therapies and Their Pharmacokinetics. *Curr. Drug Metab.* **2010**, *11*, 129−141.
(34) Avadhani, K. S.; Manikkath, J.; Tiwari, M.; Chandrasekhar, M.; Godavarthi, A.; Vidya, S. M.; Hariharapura, R. C.; Kalthur, G.; Udupa, N.; Mutalik, S. Skin Delivery of Epigallocatechin-3-Gallate (EGCG) and Hyaluronic Acid Loaded Nano-Transfersomes for Antioxidant and Anti-Aging Effects in UV Radiation Induced Skin Damage. *Drug Delivery* **2017**, *24*, 61−74.
(35) Arora, D.; Khurana, B.; Nanda, S. DoE Directed Optimization, Development and Evaluation of Resveratrol Loaded Ultradeformable Vesicular Cream for Topical Antioxidant Benefits. *Drug Dev. Ind. Pharm.* **2020**, *46*, 227−235.
(36) Ali, A.; Hassan, A.; Eissa, E.; Aboud, H. Response Surface Optimization of Ultra-Elastic Nanovesicles Loaded with Deflazacort Tailored for Transdermal Delivery: Accentuated Bioavailability and Anti-Inflammatory Efficacy. *Int. J. Nanomed.* **2021**, *16*, 591−607.
(37) Moolakkadath, T.; Aqil, M.; Ahad, A.; Imam, S. S.; Iqbal, B.; Sultana, Y.; Mujeeb, M.; Iqbal, Z. Development of Transethosomes Formulation for Dermal Fisetin Delivery: Box-Behnken Design, Optimization, In Vitro Skin Penetration, Vesicles-Skin Interaction and Dermatokinetic Studies. *Artif. Cells, Nanomed., Biotechnol.* **2018**, *46*, 755−765.
(38) Arora, D.; Khurana, B.; Nanda, S. Statistical Development and In Vivo Evaluation of Resveratrol-Loaded Topical Gel Containing Deformable Vesicles for a Significant Reduction in Photo-Induced Skin Aging and Oxidative Stress. *Drug Dev. Ind. Pharm.* **2020**, *46*, 1898−1910.
(39) Patel, R. R.; Chaurasia, S.; Khan, G.; Chaubey, P.; Kumar, N.; Mishra, B. Cromolyn Sodium Encapsulated PLGA Nanoparticles: An Attempt to Improve Intestinal Permeation. *Int. J. Biol. Macromol.* **2016**, *83*, 249−258.
(40) Elsewedy, H.; Dhubiab, B.; Mahdy, M.; Elnahas, H. Development, Optimization, and Evaluation of PEGylated Brucine-Loaded PLGA Nanoparticles. *Drug Delivery* **2020**, *27*, 1134−1146.
(41) Oseni, B.; Azubuike, C.; Okubanjo, O.; Igwilo, C.; Panyam, J. Encapsulation of Andrographolide in Poly(Lactide-Co-Glycolide) Nanoparticles: Formulation Optimization and In Vitro Efficacy Studies. *Front. Bioeng. Biotechnol.* **2021**, *9*, 639409.
(42) El Zaafarany, G.; Awad, G.; Holayel, S.; Mortada, N. Role of Edge Activators and Surface Charge in Developing Ultradeformable Vesicles with Enhanced Skin Delivery. *Int. J. Pharm.* **2010**, *397*, 164−172.
(43) Davis, M.; Chen, Z.; Shin, D. Nanoparticle Therapeutics: an Emerging Treatment Modality for Cancer. *Nanosci. Technol.* **2008**, *7*, 771−782.
(44) Sharma, D.; Maheshwari, D.; Philip, G.; Rana, R.; Bhatia, S.; Singh, M.; Gabrani, R.; Sharma, S. K.; Ali, J.; Sharma, R. K.; Dang, S. Formulation and Optimization of Polymeric Nanoparticles for Intranasal Delivery of Lorazepam Using Box-Behnken Design: In Vitro and In Vivo Evaluation. *BioMed Res. Int.* **2014**, *2014*, 156010.
(45) Ghasemian, E.; Vatanara, A.; Rouholamini Najafabadi, A.; Rouini, M. R.; Gilani, K.; Darabi, M. Preparation, Characterization and Optimization of Sildenafil Citrate Loaded PLGA Nanoparticles by Statistical Factorial Design. *Daru, J. Pharm. Sci.* **2013**, *21*, 68.
(46) Lao, L. L.; Peppas, N. A.; Boey, F. Y.; Venkatraman, S. S. Modeling of Drug Release From Bulk-Degrading Polymers. *Int. J. Pharm.* **2011**, *418*, 28−41.
(47) Kim, K. R.; You, S. J.; Kim, H. J.; Yang, D. H.; Chun, H. J.; Lee, D.; Khang, G. Theranostic Potential of Biodegradable Polymeric Nanoparticles with Paclitaxel and Curcumin Against Breast Carcinoma. *Biomater. Sci.* **2021**, *9*, 3750−3761.

https://doi.org/10.1021/acsomega.2c06359
ACS Omega 2023, 8, 976−986